# Direct Coulomb-explosion imaging of coherent nuclear dynamics induced by few-cycle laser pulses in light and heavy hydrogen

I. A. Bocharova, H. Mashiko, M. Magrakvelidze, D. Ray, P. Ranitovic, C. L. Cocke, and I. V. Litvinyuk
*J. R. Macdonald Laboratory, Physics Department, Kansas State University, Manhattan, Kansas 66506, USA*
(Received 4 March 2008; published 19 May 2008)

We followed fast evolution of coherent nuclear wave packets in $H_2$ and $D_2$ molecules after their interaction with 8-fs 800-nm laser pulses. The molecules were probed by another few-cycle pulse time delayed for up to 10 ps with respect to the pump. For neutral molecules we observed coherent rotational dynamics characterized by periodic revivals without noticeable decoherence within the 10 ps time scale. For heavy hydrogen up to four rotational states were involved in the wave packets for each of the two spin isomers. In light hydrogen the resulting dynamics was dominated by beating of just two rotational states. For neutral molecules the experimental results are in excellent agreement with our numerical simulations obtained by solving the time-dependent Schrödinger equation. By measuring time-dependent yields for singly ionized rotating $D_2$ molecules, we conclude that for an 8-fs $3\times10^{14}\,\mathrm{W/cm^2}$ pulse the ionization probability is nearly independent of the angle between the molecular axis and the electric field. For those molecules that were ionized by the pump pulse we observed both vibrational and rotational dynamics. In molecular ions coherent vibrational wave packets evolving on the bound $\sigma_g$ potential surface also exhibit revivals. Time-dependent angular distributions for the molecular ions exhibit transient alignment only soon after the pulse (18 fs for $H_2^+$ and 35 fs for $D_2^+$) with no consequent revivals within the next 10 ps due to broad distribution of active vibrational states with different rotational constants.

DOI: 10.1103/PhysRevA.77.053407 PACS number(s): 33.80.Wz, 33.15.Mt

## I. INTRODUCTION

The hydrogen molecule and its molecular ion interacting with intense laser pulses have been favorite targets for many years for both experimentalists and theorists. Even the simplest existing molecule, $H_2^+$, a seemingly uncomplicated system of two protons bound by a single electron, when put into a sufficiently strong oscillating electric field, presents researchers with an astonishing wealth of physical phenomena, such as bond softening [1], bond hardening [1,2], charge resonance enhanced ionization (CREI) [3,4], high-order harmonic generation (HHG) [5,6] and above-threshold ionization (ATI) [7] (for review see [8] and included references). This complexity stems from strong coupling between electronic and nuclear degrees of freedom and from the fundamental multiphoton nature of interactions in the strong-field regime. While over recent years many aspects of this complex behavior have been untangled to the point of at least qualitative understanding, much still remains to be done before agreement between theory and experiment could be called quantitative. These efforts are much helped by the more reliable experimental data on $H_2^+$, which is becoming available [9–11]. Nevertheless, the vast majority of experiments are still performed on neutral $H_2$ or $D_2$ targets, while fully *ab initio* calculations can only be done on their molecular ions. As a result, various empirical and semiempirical models are employed to treat the two-electron system. Disagreement between different models is not just quantitative, their conceptual bases themselves are often in clear contradiction. For instance, even qualitative interpretations of such phenomena as CREI and the recollision based "molecular clock" [12,13] remain controversial and argued about.

Understanding the behavior of molecular hydrogen is an important first step toward larger more complex molecules. In particular, uncovering detailed ionization and dissociation mechanisms will contribute to disentangling the complex pathways involved in molecular Coulomb explosion—the technique carrying some promise for dynamic imaging of molecular structure. Despite being the simplest neutral molecule, hydrogen in one sense is more challenging to study experimentally than larger molecules—its nuclei are the lightest and their motion is the fastest. A strong oscillating electric field directly affects only electrons, but their motion is very efficiently coupled into rotational (by anisotropic polarizability) and vibrational (by $R$-dependent dipole moment and ionization rate) nuclear degrees of freedom. As a result a nonresonant laser pulse causes vibrational and rotational excitation of the molecule. Moreover, the excitations are produced within a range of vibrational and rotational states with definite relative phases, resulting in coherent vibrational and rotational wave packets. Classically, those wave packets can be viewed as very fast axial and angular motions of the molecule. For instance, it takes only about 10 fs for a vibrational wave packet generated by ionization of a neutral molecule and moving on the ground-state potential energy surface of $H_2^+$ to reach its outer turning point. It may take as little as 20 fs for a hydrogen molecule excited by a laser pulse to rotate by 90°. Therefore, with pulses of 20 fs and longer a hydrogen molecule may undergo a wide range of motion during the pulse, obscuring any possible effects differential in respect to internuclear separation or molecular alignment. Laser pulses which are shorter than 10 fs are needed to efficiently generate fast vibrational and rotational wave packets and to detect and measure their properties in a time-resolved way.

After it was first demonstrated that few-cycle 800-nm laser pulses can effectively "freeze" vibrational motion in $H_2$ [14], a series of pump-probe experiments have traced time

 

evolution of nuclear wave packets generated by ionization of neutral hydrogen on the ground ($\sigma_g$) and first excited ($\sigma_u$) potential energy surfaces of $H_2^+$ [15,16] and even in the ground state of the neutral molecule itself [17]. Those experiments focused on vibrational motion of the nuclei. It was also shown that femtosecond pulses generate coherent rotational wave packets in $D_2$ [18–20] and $H_2$ [20]. Coherent rotational wave packets are used successfully to perform strong-field experiments on transiently aligned molecules (field-free alignment) and to measure such angle-dependent parameters as ionization rates [21,22], HHG yields [23,24] and electron momentum distributions [25]. While all larger linear molecules can be aligned efficiently using this technique, hydrogen and deuterium are much harder to align due to their low polarizability anisotropy and low rotational inertia (large energy separation between rotational levels). Therefore, extracting parameters differential in respect to the molecular angle remains problematic for these lightest molecules. For instance, it remains unknown how different the ionization rates are for hydrogen molecules aligned parallel and perpendicular to the laser polarization.

Here we present a study of nuclear dynamics induced in $H_2$ and $D_2$ by 8-fs 800-nm laser pulses. We probed fast nuclear motion by exploding the molecule with another more intense time-delayed few-cycle pulse and measuring the three-dimensional (3D) momenta of the resulting fragments. We specifically focused on rotational motion of these molecules, having followed it for up to 10 ps in time delay. This paper is presented as follows: First we briefly describe our experimental setup and procedure; that is followed by the main section presenting and discussing our results; then, after some concluding remarks and acknowledgments, an Appendix describes the numerical simulations for rotations of neutral molecules. In the main section we present time-resolved kinetic energy release (KER) spectra and explain how we separate rotational dynamics in neutral molecules from that of molecular ions. Then we focus on rotational motion of $H_2$, $D_2$, $H_2^+$, and $D_2^+$. We present and discuss measured time traces of $\langle \cos^2 \theta \rangle$—a parameter characterizing molecular alignment. For neutral molecules we also show experimental angular distributions at different points in the evolution of coherent rotational wave packets. Based on these distributions, and on measured time-dependent yields for single ionization channels of $D_2$, we set an upper limit on the strong-field ionization anisotropy of this molecule and conclude that its ionization is nearly isotropic under conditions used in our experiment. The main section is concluded by discussion of rotational dynamics observed in molecules which have been ionized by the pump pulse.

## II. EXPERIMENTAL SETUP

Our experimental setup is schematically shown in Fig. 1. The few-cycle near-ir laser pulses were generated by compressing the output of a Ti:sapphire amplifier (35 fs, 1 mJ, 1 kHz repetition rate) with an Ar-filled hollow-core fiber (400 $\mu$m diameter, 650 torr pressure [26]) compressor and a set of chirped mirrors (7 Femtolaser and 4 Layertec) to yield 8 fs pulses of 400 $\mu$J energy. The pulse duration was confirmed with frequency-resolved optical gating (FROG) measurement as well as by autocorrelation measuring the ion yield inside the chamber. Stability of the few-cycle pulse duration was monitored throughout the experiment by checking the kinetic energy spectra of the $D^+$ fragments: Few-cycle pulses suppress the enhanced ionization channel resulting in more energetic $H^+$ and $D^+$ fragments [14]. The total pulse energy was controlled by using a reflective polarizer (two germanium plates at the Brewster angle) in fixed position and rotating the polarization of the 35-fs pulse before the fiber. Two replicas of the pulse with a variable delay were produced with a Mach-Zehnder interferometer using a pair of thin broadband beam splitters (Femtolaser) and a motorized translation stage (Thorlabs). The diameter of the pump beam was further restricted by an iris to decrease its intensity and increase its focal volume in comparison to that of the probe pulse. For most experiments the pump and probe pulses were polarized collinearly.

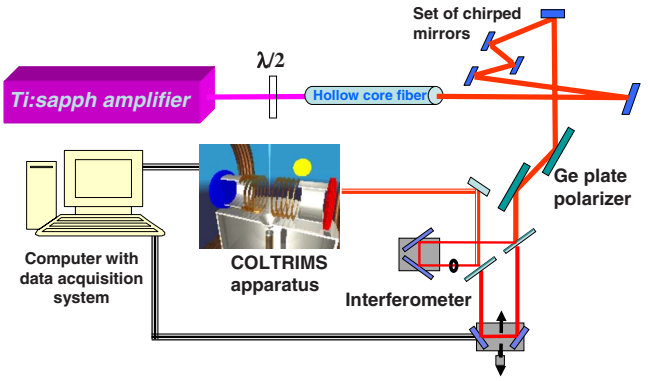


FIG. 1. (Color online) Schematic of the experimental setup.

The pulses were focused by an on-axis spherical mirror ($d$=25 mm, $f$=75 mm) on a supersonic jet of target molecules in the interaction region of a COLTRIMS apparatus. The resulting ion fragments were extracted by a uniform electric field (35 V/cm) and detected by a time- and position-sensitive delay-line-anode detector (Roendtek with LeCroy 3377 TDC-0.5 ns time and 0.25 mm position resolution). From position and time of impact full 3D momentum of each ion fragment can be reconstructed. The laser polarization was along the extracting electric field and perpendicular to the molecular jet propagation direction. We measured the translational temperature of the jet to be about 110 K in the longitudinal direction by measuring momentum distributions of $D_2^+$ molecular ions. In the transverse direction the jet is cooled geometrically to a few mK temperature. The temperature of background $H_2$ also used in the experiments was measured to be 295 K. We determined the laser peak intensity *in situ* by measuring momentum distributions of $Ar^+$ ions produced by a circularly polarized pulse, as described in [27]. To produce circular polarization an achromatic quarter-wave-plate (CVI) was introduced instead of a corresponding amount of fused silica which did not affect the pulse duration. The measured intensity agreed well with the one estimated from the pulse energy, duration, and beam diameter.

## III. RESULTS AND DISCUSSION

Nuclear dynamics in $H_2$ and $D_2$ was initiated by an 8-fs pump pulse of peak intensity of $1.0 \times 10^{14}$ W/cm$^2$. At this

intensity only a small fraction of molecules within the interaction region is ionized at the peak of the pulse. In such molecules a coherent vibrational wave packet is launched on the ground electronic state ($\sigma_g$) potential energy surface of the molecular ion. Consequently, at the tail of the pump pulse this wave packet can be promoted to the lowest excited state ($\sigma_u$) which is repulsive, leading to dissociation of the molecule. However, the majority of the molecules remain neutral and experience only rotational excitation. The dynamics following the pump pulse is interrogated by a time-delayed probe pulse of the same duration but higher intensity ($3\times10^{14}$ W/cm$^2$). This intensity is sufficient to ionize most neutral molecules at least singly (dissociating some of them), to remove the remaining electron from molecular ions produced by the pump pulse, and to doubly ionize a significant fraction of neutrals. Doubly ionized molecules will undergo immediate Coulomb explosion, with the resulting KER closely mapping the internuclear distance at which the last electron was removed. At the same time the direction of the fragments' momenta reflects the direction of internuclear axes at the same moment. Thus, time-dependent KER spectra image vibrational (and dissociative) motion of the molecule, while time dependence of angular distributions reflects its rotational dynamics.

### A. Coherent vibrational dynamics in $D_2^+$

Figure 2 presents time-dependent KER spectra for $D^+$ (showing the sum energy for two fragments) in the time interval from −200 fs to 1200 fs. Most of the $D^+$ signal falls within the 9–15 eV energy band and does not exhibit any time dependence. That corresponds to sequential double ionization of neutral $D_2$ by a few-cycle pulse, when the enhanced ionization process (~5 eV energy) is suppressed. In addition one can see both vibrating and dissociating wave packets launched by the pump in $D_2^+$. To better reveal that dynamics, the time-independent part can be easily subtracted from the KER spectra. The dissociating wave packet results in a trace of monotonically decreasing kinetic energy which asymptotically approaches 1.2 eV—the ultimate energy of the dissociation fragments, as Coulomb repulsion adds nothing to this energy when the second ionization takes place at very large distances. The dissociation is mostly complete within 100 fs. The bound vibrational wave packet undergoes a few quasiperiodic oscillations, before anharmonicity of the potential causes it to dephase. After about 600 fs the wave packet experiences a revival, followed by another one 600 fs later, as was predicted theoretically [28] and was seen in previous experiments [29]. The spectra at negative delays represent the case of reverse order of pulses—when the more intense pulse serves as a pump. We did not follow it past 200 fs delays, but within that range the general features of the dynamics are similar to the weaker pump—stronger probe case, though the branching ratio between the bound and dissociating states is obviously changed in favor of dissociation.

### B. Coherent rotational dynamics in neutral molecules

To image the rotational motion we measured time-dependent angular distributions of fragments. In the first approximation angular distributions can be characterized by a single parameter-$\langle\cos^2\theta\rangle$-average squared cosine of the angle $\theta$ between the molecular axes and a preferred direction (in our case the polarization direction of the pump pulse). To separate rotational dynamics of neutral molecules from that of molecular ions we put a gate on kinetic energy of the fragments: The 9–15 eV fragments are dominated by exploding neutrals, while the 5–9 eV fragments come mostly from the ions which are typically ionized the second time at larger internuclear distances. Even for short 8-fs linearly polarized probe pulses the Coulomb explosion process itself is not isotropic: When applied to an initially isotropic ensemble of molecules it produces a fragment angular distribution biased toward the laser polarization direction. This bias is caused by a combination of factors: A possible angular dependence of both ionization steps and also of the intermediate nuclear dynamics (so-called geometric alignment); rotation of molecular axis toward the polarization direction during the pulse before the explosion (dynamic alignment); and limited validity of the axial recoil approximation for fast rotating molecules (post-ionization alignment [30]). The relative im-

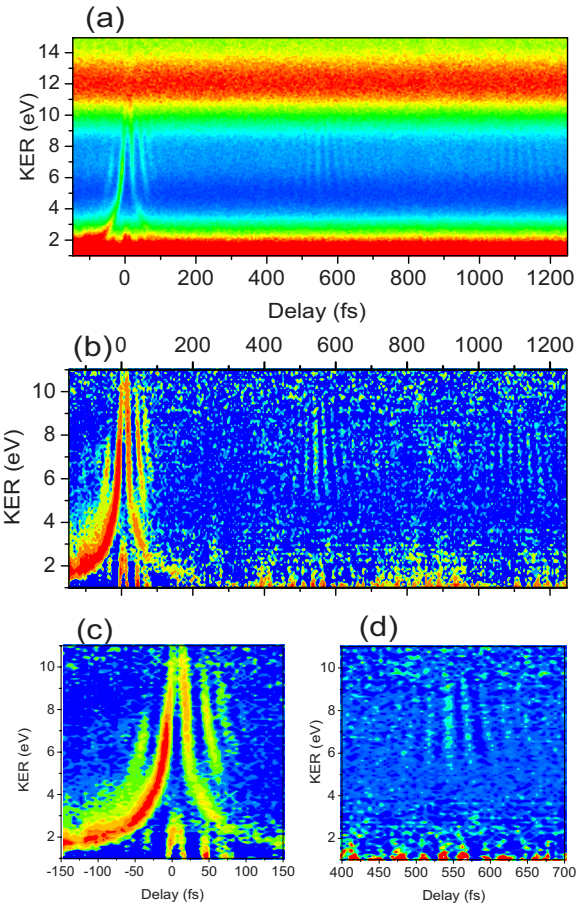


FIG. 2. (Color online) Time-dependent KER spectra for $D_2$. Pump pulse −8 fs $1\times10^{14}$ W/cm$^2$; probe pulse −8 fs $3\times10^{14}$ W/cm$^2$. Panel (a) shows full spectrum including the time-independent 9–16 eV band resulting from the probe exploding the neutral $D_2$ molecules. Panel (b) shows KER for the molecules ionized by the pump—time-independent band is subtracted. (c) and (d) same as (b) focusing on dynamics at short pump-probe delays and around the vibrational revival time.

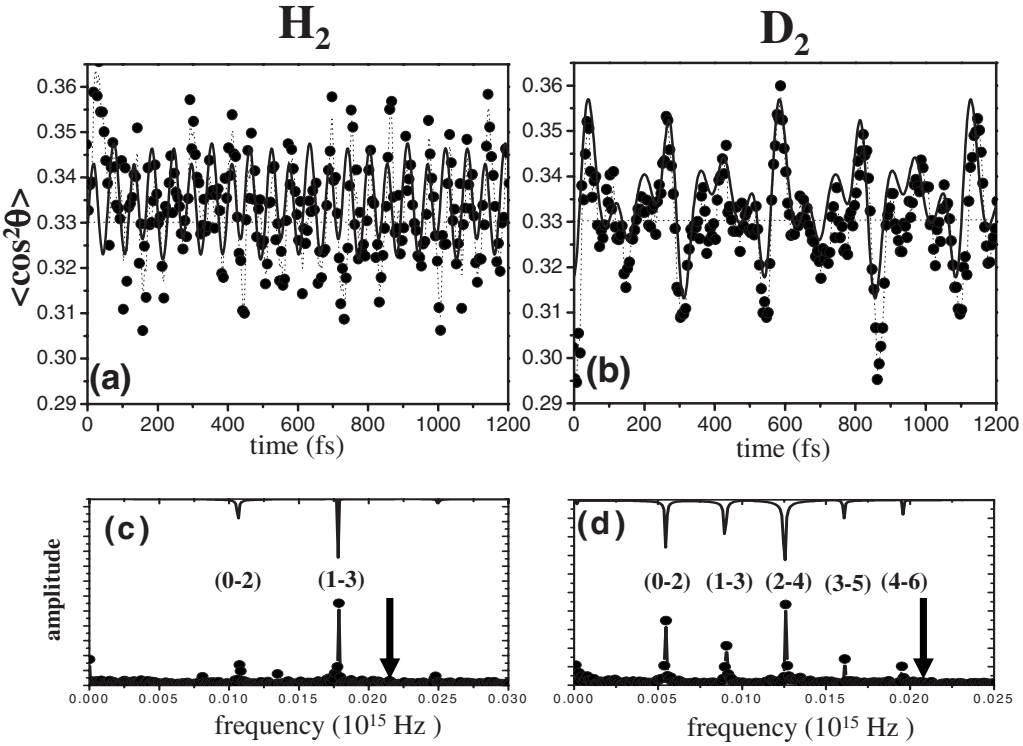


FIG. 3. Rotational dynamics of neutral $H_2$ and $D_2$: (a) and (b) Measured (symbols and dotted line) and calculated (solid line) time traces of $\langle \cos^2 \theta \rangle$ (see text for details) for $H_2$ and $D_2$; (c) and (d) Fourier spectra of measured (with symbols) and calculated (inverted scale) time traces of $\langle \cos^2 \theta \rangle$ for $H_2$ and $D_2$. Each line corresponds to a $(J, J+2)$ energy difference as indicated. Arrows represent the spectral bandwidth of an 8-fs laser pulse. Simulations used 10-fs $1 \times 10^{14}$ W/cm$^2$ pulses. Initial rotational temperature was taken to be 250 K for $D_2$ and 295 K for $H_2$.

portance of those factors for hydrogen Coulomb explosion is still being debated. In our analysis we accounted for this bias by normalizing the measured angular distributions to those obtained with probe pulses alone, so that after the normalization an isotropic ensemble of molecules would yield an isotropic distribution of fragments with $\langle \cos^2 \theta \rangle = 1/3$.

The time dependence of $\langle \cos^2 \theta \rangle$ for normalized angular distributions of neutral $D_2$ and $H_2$, isolated by limiting the KER to 9–15 eV, is shown in Fig. 3. The trace is typical of coherent rotational wave packets with characteristic periodic revivals and alternating states of alignment and antialignment. For $D_2$ the full rotational period is 558 fs, while for $H_2$ it is one-half of that (279 fs). The figure presents only the 0–1200 fs delay-time range to emphasize the main features of the dynamics. This pattern repeats itself periodically up to 10 ps of delay without any signs of decoherence. These coherent rotational wave packets can be interpreted as very fast classical rotations of the molecular axes: It takes only 30 fs for $H_2$ and 40 fs for $D_2$ to rotate by 90° (from alignment to antialignment). Although the range of change for $\langle \cos^2 \theta \rangle$ is almost the same (0.30–0.36) for light and heavy molecules, for $D_2$ the revivals look more like those seen in heavier molecules ($O_2$ and $N_2$ [31]), while for $H_2$ they more resemble a beating pattern. The Fourier transform of the two time traces emphasizes the difference. Each narrow line in the Fourier spectrum corresponds to an energy difference between a pair of rotational states with rotational quantum numbers $J$ and $J+2$. For $H_2$ the spectrum is dominated by just two lines—(0–2) and (1–3). Each of them is associated with a particular nuclear spin isotope of light hydrogen: Ortho-$H_2$ is allowed only odd $J$ states, para-$H_2$ is allowed only even $J$ states. The statistical ortho-para ratio (3:1) is reflected in the relative heights of the two lines. Obviously, in each $H_2$ spin form the rotational wave packets consist of just the two lowest rotational states beating with each other. In contrast, the $D_2$ Fourier spectra contain more lines: Three for ortho-$D_2$ (0–2, 2–4, and 4–6) and two for para-$D_2$ (1–3 and 3–5) resulting in better defined wave packets and revivals. The statistical ratio (also reflected in the spectrum) of ortho-to-para-$D_2$ is 2:1, with the ortho form associated with even $J$'s.

The difference between the light and heavy molecules is easy to understand in terms of energy separation between the adjacent $J$ and $J+2$ rotational levels. The energy separation is two times as large for $H_2$, making rotational excitation through a sequential nonresonance stimulated Raman process more difficult. For both $H_2$ and $D_2$ the rotational level spacing is much larger than for any other molecule, making them particularly hard to align. For a stimulated Raman transition between two levels to occur efficiently their energy difference must not exceed the bandwidth of the laser pulse, which must contain both up and down transition frequencies. The bandwidth of an 8 fs pulse is given by the uncertainty principle as $\Delta\nu \cdot (8 \text{ fs}) \geq (2\pi)^{-1}$ as $\Delta\nu = 0.02 \times 10^{15}$ Hz, which corresponds to the cutoff frequency in the Fourier spectra for both $H_2$ and $D_2$. It appears that, quite counterintuitively, even shorter pulses (or non-transform-limited pulses with a broader bandwidth) are needed to better align hydrogen.

We simulated rotational dynamics of neutral $H_2$ and $D_2$ molecules by solving the time-dependent Schrödinger equation for a rigid rotor coupled to the field by anisotropic polarizability (see the Appendix for details). The calculated $\langle \cos^2 \theta \rangle$ traces and Fourier spectra are in excellent agreement with our experimental results, when we use a Gaussian pulse of 10 fs [intensity full width at half-maximum (FWHM)] duration and $1 \times 10^{14}$-W/cm$^2$ peak intensity. However, to reproduce our experimental results well we had to take the initial rotational temperature of $D_2$ to be 250 K or higher. That is more than 2 times as hot as the measured translational temperature of our $D_2$ jet (110 K) and only slightly cooler than the room temperature. We conclude that our weakly supersonic molecular jet does not efficiently cool rotational motion of $D_2$, "freezing" it in a non-Boltzmann distribution with high effective temperature. The large rotational energy level spacing is also responsible for that. We used Boltzmann distribution of initial rotational states in our calculations.

The experimental angular distributions measured for neutral $D_2$ molecules at the times of maximum alignment and antialignment are shown in Fig. 4. They can be well approximated by the formula

$$\Pi(\theta) = \frac{3}{4\pi(1+2\varepsilon)}(\cos^2 \theta + \varepsilon \sin^2 \theta), \quad (1),$$

where $\Pi(\theta)$ is the probability (per unit solid angle) that the molecular axis makes angle $\theta$ with laser polarization, parameter $\varepsilon$ describes the ratio of the probabilities for a molecule to be perpendicular and parallel to the laser polarization, and the normalization factor is selected so that $2\pi \int_0^\pi \Pi(\theta) \sin \theta d\theta = 1$. For angular distribution (1)

$$\langle \cos^2 \theta \rangle = \frac{2\varepsilon + 3}{5(2\varepsilon + 1)}.$$

The value of $\varepsilon$ corresponding to alignment (antialignment) is 0.75 (1.5) meaning that the ratio of probabilities changes by a factor of 2 as the wave packets evolve.

### C. Angular dependence of ionization for neutral $D_2$

It is interesting to use anisotropic angular distributions in order to estimate anisotropy of strong-field ionization rates for $D_2$. It has been predicted theoretically [32] and demonstrated experimentally [21,22,33] that for most linear molecules ionization rates (probabilities) strongly depend on molecular orientation with respect to the laser electric field vector, with this angular dependence reflecting the symmetry of the corresponding molecular orbital. For instance, $N_2$ is more likely to ionize when it is parallel to the electric field, while for $O_2$ the ionization probability is the largest for about 45° angle. It is important to know this ionization anisotropy in order to calculate total ionization rates for isotropic molecular gases, to fully understand strong-field experiments performed on prealigned molecules and to judge the validity of various theoretical models. It is of particular interest for $D_2$, as this molecule exhibits significant suppression of ionization rates in comparison to Ar (which has similar ionization potential). Various theories disagree on this issue, with MO-ADK predicting almost no anisotropy [32] and other theories finding significant angular dependence [34]. To shed some light on this issue we followed time-dependent yields for different ionization channels of rotating $D_2$ molecules. Figure 5 presents the measured yields for $D_2^+$ and $D^+ + D$ channels, as well as their correlation with values of $\langle \cos^2 \theta \rangle$. The yield of the Coulomb explosion ($D^+ + D^+$) channel (not shown) did not exhibit any correlation with $\langle \cos^2 \theta \rangle$, while the two single ionization channels do correlate with molecular alignment. The yield of an intact molecular ion correlates negatively—less $D_2^+$ is produced when neutral molecules are aligned along the laser electric field. At the same time the ($D^+ + D$) channel correlates positively—more low-energy (0

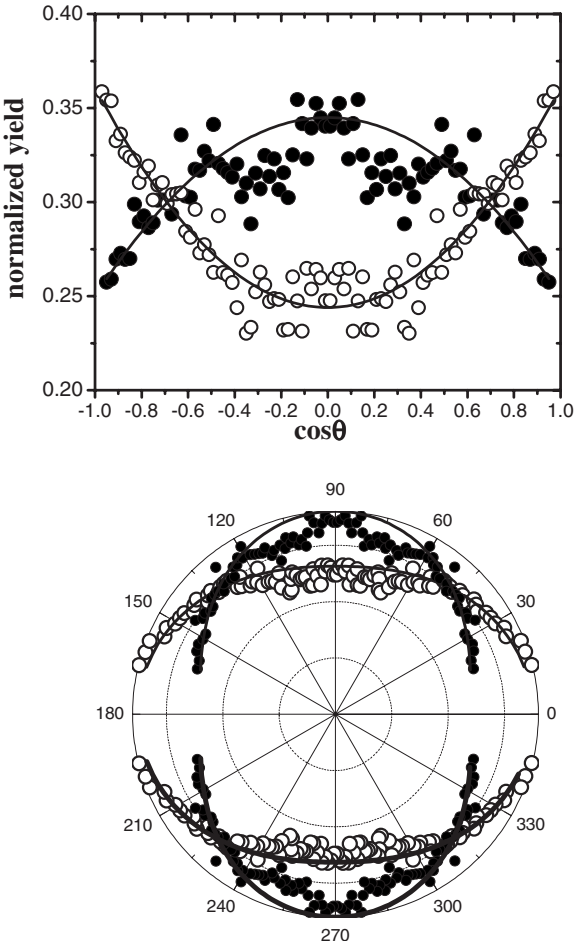


FIG. 4. Experimental angular distributions measured for $D_2$ at the times of maximum alignment (hollow circles) and antialignment (filled circles). Normalized relative yields (per unit solid angle) for $D^+ + D^+$ channels (9 eV < KER < 18 eV) are shown as functions of $\cos \theta$ and $\theta$, where $\theta$ is the angle between molecular axis (momentum vector of $D^+$) and polarization direction of the aligning pulse. To improve statistics, momentum angles for uncorrelated $D^+$ ions with energies 4.5–9 eV were measured. Only $D^+$ ions initially flying away from the detector were considered in order to exclude overlapping backward $H^+$ signal from background $H_2$. The resulting distributions were symmetrically reflected into the other hemisphere. Solid lines show fits with the function $(\cos^2 \theta + \varepsilon \sin^2 \theta)$: $\varepsilon = 0.75$ for aligned and $\varepsilon = 1.5$ for antialigned distributions.

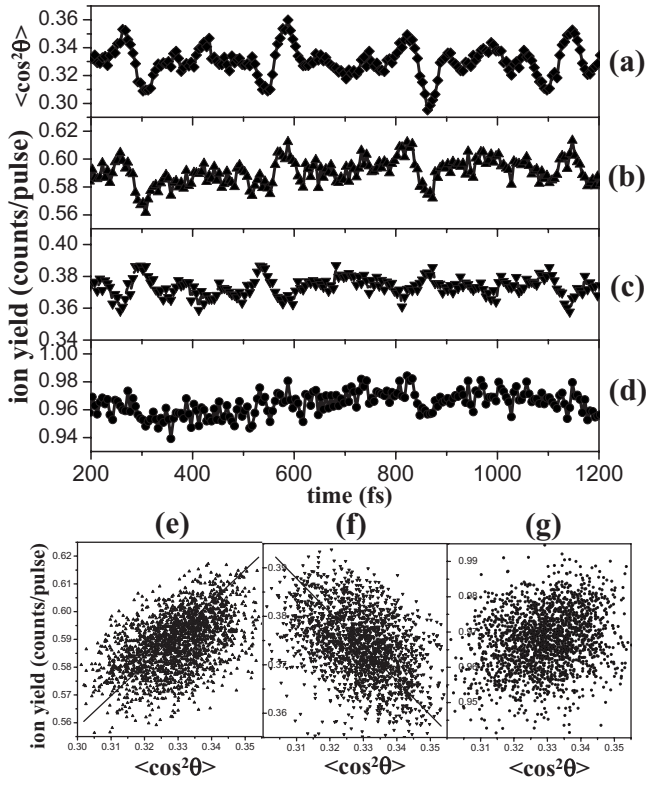


FIG. 5. Time-dependent yields for single ionization channels of rotating neutral $D_2$: (a) Alignment parameter $\langle \cos^2 \theta \rangle$; (b) yield for the bond softening ($D^+ + D$) channel; (c) yield for the molecular ion ($D_2^+$); (d) total yield for both single ionization channels; (e), (f), and (g) correlation graphs between $\langle \cos^2 \theta \rangle$ and time-dependent yields for ($D^+ + D$), $D_2^+$ and total single ionization of $D_2$, respectively.

to 2 eV) deuterons are produced when molecules are aligned. Together these two channels represent single ionization of $D_2$ by the probe pulse. Some molecular ions remain bound, while others are dissociated by the same pulse through laser-induced bond softening. The bond softening process is known to be very strongly anisotropic—the required field coupling of $\sigma_g$ and $\sigma_u$ electronic states is the strongest for molecules aligned along the field. Therefore, it is not surprising that at times of maximum alignment more molecular ions are lost to bond softening than for antialigned distributions. On balance, variations of the two single ionization channels almost cancel each other out, with a very small positive correlation (yield variation $\leqq 1.5\%$) remaining for total singly ionized $D_2$ yield.

Based on these results and experimental angular distributions we can put an upper limit on the ionization anisotropy of $D_2$. To do this we assume that the anisotropic ionization probability is represented by $P(\theta) \sim \cos^2 \theta + e \sin^2 \theta$, where $\theta$ is the angle between the molecular axis and the laser electric field vector and parameter $e$ represents the ratio of probabilities for molecules aligned perpendicular and along the field. The total ionization signal can be found as $S \sim \int_0^{\pi} P(\theta) \Pi(\theta) \sin \theta d\theta$, where $\Pi(\theta)$ is the angular distribution of molecular axes, which is assumed to be axially symmetric around the polarization (alignment) direction. We also assume that the probe pulse itself does not affect angular

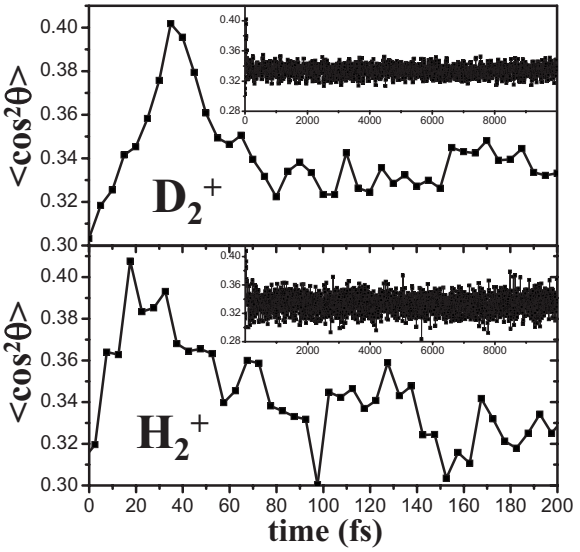


FIG. 6. Rotational dynamics of $D_2^+$ and $H_2^+$ ions produced by the pump: Time traces for $\langle \cos^2 \theta \rangle$ measured using fragments with $4\ \text{eV} < \text{KER} < 9\ \text{eV}$. Insets represent the full experimental delay time range of $0-10\,000$ fs.

distributions much, which seems reasonable with 8 fs pulse duration being less than 40 fs taken by molecules to rotate by 90°. For angular distributions of molecular axes given by (1) the total ionization signal depends on both anisotropies ($\varepsilon$ of the angular distribution and $e$ of the ionization probability) as

$$S(\varepsilon, e) \sim \frac{3 + 2e + 2\varepsilon + 8e\varepsilon}{5(1 + 2\varepsilon)}.$$

Using this formula we can put a lower limit of 0.8 on the value of $e$ consistent with our data, meaning that with our experimental conditions $D_2$ molecules aligned along the laser electric field have at the most 1.25 higher probability to be ionized than those aligned perpendicular to the field. Thus, strong field ionization of $D_2$ appears to be nearly isotropic. However we must note that in our experiments the probe pulse peak intensity ($3 \times 10^{14}$ W/cm$^2$) was fairly close to saturation intensity and the anisotropy may be much higher for weaker pulses.

### D. Rotation of molecular ions

We also followed rotational dynamics of molecules which are ionized by the pump pulse. They are characterized by lower KER since the second ionization by the probe typically happens at larger internuclear distances. We plotted $\langle \cos^2 \theta \rangle$ for $H^+$ and $D^+$ fragments with KER between 5 and 9 eV (Fig. 6). Unlike the rotational wave packets in neutral molecules, the rotational dynamics in molecular ions does not exhibit periodic coherent behavior. There is a prompt alignment immediately after the pulse, much stronger than in the neutrals, which very quickly dephases and never revives within our 10 000 fs experimental time scale. The maximum degree of alignment is reached 18 fs after the peak of the pump pulse for $H_2^+$ and 35 fs after the pulse for $D_2^+$. These times are relevant for understanding the dynamics of Coulomb explo-

sion of hydrogen by femtosecond laser pulses, in particular the issue of dynamic versus geometric alignment of molecules during the pulse. Our data indicate that $H_2^+$ can be aligned in just 18 fs, while it takes two times as long to align the heavier $D_2^+$. Therefore, for pulses of about 15 fs duration and more for $H_2$ and 30 fs and more for $D_2$ alignment during the pulse will contribute significantly to the overall dynamics of the molecule-field interactions. The absence of prominent rotational revivals in the ions is due to the broad distribution of vibrational states resulting from strong field ionization of neutral molecules. An exact form of that vibrational distribution is a matter of great interest in its own right, with the scarce experimental data [35] indicating that it is a strongly non-Frank-Condon one. Each of the vibrational states forming the wave packet has a different rotational constant (and time) and in its pure form would revive at a different time. Instead of a rigid rotor (as in the case of a neutral molecule) we have a rotor with time-dependent fast-varying rotational constant, resulting in quasichaotic rotational motion. Due to that coupling of vibrations and rotations, the vibrational frequency differences seen in time-dependent KER spectra [36] also appear in Fourier transforms of time-dependent $\langle \cos^2 \theta \rangle$ traces for $D_2^+$. It is interesting to note that if instead of a coherent vibrational wave packet one looked at an incoherent superposition of vibrational states (as in ions coming, for instance, from an ion source) one would expect to see coherent rotational motion again, with revivals at regular intervals determined by a rotational constant describing the averaged time-independent distribution of internuclear distances for those ions.

## IV. CONCLUDING REMARKS

In summary, we reported a direct time-resolved Coulomb explosion imaging experiment following coherent nuclear dynamics induced by a few-cycle near-ir laser pulse in $D_2$ and $H_2$. In neutral molecules the rotational dynamics is that of a rigid rotor coupled to the electric field by its anisotropic polarizability. As in larger diatomics, periodic rotational revivals corresponding to partial alignment of molecular axes are seen in both light and heavy hydrogen. However, the degree of alignment is quite low for both ($\langle \cos^2 \theta \rangle \approx 0.36$) due to large energy spacing between the rotational levels of the two molecules. This large rotational level spacing is also the reason for inefficient rotational cooling of $D_2$ in a supersonic jet. We found that the effective rotational temperature in our jet is 250 K, while the translational temperature was 110 K. We do not believe, however, that high initial rotational temperature was the main reason for poor alignment. Much more important, even few-cycle pulses do not have sufficient spectral bandwidth to excite the high rotational states needed to produce well-localized wave packets in both $H_2$ and $D_2$. At the most, states with $J=3$ in $H_2$ and $J=6$ in $D_2$ can be efficiently excited by a nonresonant stimulated Raman process using 8 fs pulses. That puts a natural limit on the degree of field-free alignment achievable in molecular hydrogen with short single-color pulses and calls for development of other more efficient methods in order to experimentally study its angle-differential properties. One possible solution may involve using two-color aligning pulses (for instance, $\omega+2\omega$) with a much broader combined spectrum. Despite the relatively poor alignment we were able to put an upper limit of 1.25 on the ratio of ionization probabilities for $D_2$ molecules aligned along and perpendicular to the laser electric field. Strong-field ionization of $D_2$ appears to be nearly isotropic in agreement with predictions of the molecular ADK theory.

In molecular ions we observed coupled rovibrational dynamics. Only vibrational revivals were seen in $D_2^+$. Within the 10-ps experimental time scale, rotational motion of $D_2^+$ and $H_2^+$ did not exhibit any coherence beyond the initial prompt alignment immediately after the pulse. That alignment occurred very fast (18 fs in $H_2^+$ and 35 fs in $D_2^+$) and was much better defined than in neutral molecules. The absence of revivals is not at all surprising, since different vibrational states forming the coherent wave packet have very different and incommensurate rotational times. To fully understand nuclear wave-packet dynamics in hydrogen molecular ions one must treat the coupled vibrational and rotational degrees of freedom simultaneously, particularly with both motions taking place on a very similar time scale. Properly taking rotations into account may resolve the remaining discrepancies between the experimental results and one-dimensional vibrations-only model calculations [36].

## ACKNOWLEDGMENTS

The authors gratefully acknowledge invaluable help from Professor Zenghu Chang and Al Rankin in operating the laser source. We are also grateful to Professor Brett Esry and Fatima Anis for advice and help with the theory and to Carol Regehr. This work was supported by funding from Chemical Sciences, Geosciences and Biosciences Division, Office of Basic Energy Sciences, Office of Science, U.S. Department of Energy.

## APPENDIX: NUMERICAL SIMULATIONS

The calculations are similar to those described in [31]. First, we numerically solve the time-dependent Schrödinger equation which describes interaction of a neutral molecule in the ground vibrational state with a laser pulse through the nonresonant ac Stark shift

$$i\dot{\psi}(\vartheta,t) = [B\mathbf{J}^2 - U(t)\cos^2\vartheta]\psi(\vartheta,t),$$

where $\theta$ is the angle between the laser field polarization direction and the molecular axis, $\mathbf{J}$ is the angular momentum operator, $B$ is the rotational constant of the molecule, and $U(t)$ is the effective time-dependent interaction potential,

$$U(t) = -\frac{1}{4}(\alpha_\perp + \Delta\alpha \cos^2 \vartheta)E^2(t),$$

$$E^2(t) = E_0^2 \exp\left(-4 \ln(2)\frac{(t-t')^2}{\tau^2}\right),$$

where $\Delta\alpha$ and $\alpha_\perp$ are the polarizability anisotropy and the polarizability component perpendicular to the molecular

axis, and $E(t)$ is the electric field strength which is taken in the shape of a Gaussian pulse envelope of duration $\tau$. We used the same pulse peak intensity and duration which were estimated for the actual pulse in our experiments. Numerical integration of the TDSE by the finite differences method is done in the basis of rotational eigenstates of the rigid rotor $|J,M\rangle$ over the time interval of $10\tau$ centered on the peak of the pulse. Starting with a pure single rotational state the integration yields populations and phases of all rotational states involved in the resulting coherent superposition

$$\psi_0 = \sum_J a_J |J,M\rangle,$$

where $a_J$ are the complex amplitudes for each rotational state. This wave packet is then subjected to field-free evolution,

$$\psi(t) = \sum_J a_J e^{-i(E_J/h)t} |J,M\rangle,$$

$$E_J = BJ(J+1) - D[J(J+1)]^2,$$

where $E_J$ are the energies of a rotor including the centrifugal distortion term. To compare the simulation to our experimental data we extracted the same observable that we measured—$\langle \cos^2 \theta \rangle$ the average cosine squared of the angle between the molecular axis and the polarization direction of the pulse,

$$\begin{aligned}\langle \cos^2 \vartheta \rangle &= \langle \psi(t) | \cos^2 \vartheta | \psi(t) \rangle \\ &= \sum [|a_J|^2 C_{J,J,M} + |a_J||a_{J+2}| \cos(\Delta\omega_{J,J+2} t \\ &\quad + \varphi_{J,J+2}) C_{J,J+2,M}],\end{aligned}$$

$$C_{J,J,M} = \langle J,M | \cos^2 \vartheta | J,M \rangle,$$

$$C_{J,J+2,M} = \langle J,M | \cos^2 \vartheta | J+2,M \rangle,$$

where $\phi_{J,J+2}$ is the phase difference between the $J$ and $J+2$ states at the start of the evolution, and $\Delta\omega_{J,J+2}$ are the frequency differences between rotational states characterized by rotational quantum numbers $J$ and $J+2$.

To account for a finite initial rotational temperature of the target we summed the results obtained for different initial rotational states weighted by the Boltzmann population of each state for a given rotational temperature,

$$\langle \cos^2 \vartheta \rangle_T = \sum_J \frac{\exp\left(-\frac{E_J}{kT}\right)}{Q} \sum_M \langle \cos^2 \vartheta \rangle_{J,M},$$

where $Q$ is the partition function. The thermal averaging is done separately for each spin form (ortho and para) of $H_2$ and $D_2$, with each form being allowed only even or odd values of $J$. Thus, for $H_2$ (nuclear spin-$\frac{1}{2}$) ortho form (total spin-1) can be only in $J=1,3,5,\ldots$ and para (total spin $-0$) in $J=0,2,4,\ldots$, with ortho-to-para ratio of 3:1. For $D_2$ (nuclear spin $-1$) ortho form (total spin $-0$ or 2) can be in even $J$ states, while para (total spin $-1$) only in odd $J$ states, with ortho-to-para ratio of 2:1. Contributions from ortho- and para-spin forms were added together with proper weights for $H_2$ and $D_2$, to produce the calculated traces of $\langle \cos^2 \theta \rangle$.


[1] P. H. Bucksbaum, A. Zavriyev, H. G. Muller, and D. W. Schumacher, Phys. Rev. Lett. **64**, 1883 (1990).

[2] A. D. Bandrauk and M. L. Sink, J. Chem. Phys. **74**, 1110 (1981).

[3] T. Zuo and A. D. Bandrauk, Phys. Rev. A **52**, R2511 (1995).

[4] T. Seideman, M. Y. Ivanov, and P. B. Corkum, Phys. Rev. Lett. **75**, 2819 (1995).

[5] Y. Liang, S. Augst, S. L. Chin, Y. Beaudoin, and M. Chaker, J. Phys. B **27**, 5119 (1994).

[6] S. Baker, J. S. Robinson, C. A. Haworth, H. Teng, R. A. Smith, C. C. Chirilă, M. Lein, J. W. G. Tisch, and J. P. Marangos, Science **312**, 424 (2006).

[7] A. Zavriyev, P. H. Bucksbaum, H. G. Muller, and D. W. Schumacher, Phys. Rev. A **42**, 5500 (1990).

[8] J. H. Posthumus, Rep. Prog. Phys. **67**, 623 (2004).

[9] D. Pavicic, A. Kiess, T. W. Hansch, and H. Figger, Phys. Rev. Lett. **94**, 163002 (2005).

[10] I. D. Williams, P. McKenna, B. Srigengan, I. M. G. Johnston, W. A. Bryan, J. H. Sanderson, A. El-Zein, T. R. J. Goodworth, W. R. Newell, P. F. Taday, and A. J. Langley, J. Phys. B **33**, 2743 (2000); J. McKenna, M. Suresh, D. S. Murphy, W. A. Bryan, L.-Y. Peng, S. L. Stebbings, E. M. L. English, J. Wood, B. Srigengan, I. C. E. Turcu, J. L. Collier, J. F. McCann, W. R. Newell, and I. D. Williams, *ibid.* **40**, 2607 (2007).

[11] I. Ben-Itzhak, P. Q. Wang, J. F. Xia, A. M. Sayler, M. A. Smith, K. D. Carnes, and B. D. Esry, Phys. Rev. Lett. **95**, 073002 (2005); P. Q. Wang, A. M. Sayler, K. D. Carnes, J. F. Xia, M. A. Smith, B. D. Esry, and I. Ben-Itzhak, Phys. Rev. A **74**, 043411 (2006).

[12] H. Niikura, F. Legare, R. Hasbani, A. D. Bandrauk, M. Y. Ivanov, D. M. Villeneuve, and P. B. Corkum, Nature (London) **417**, 917 (2002); H. Niikura, F. Legare, R. Hasbani, M. Y. Ivanov, D. M. Villeneuve, and P. B. Corkum, *ibid.* **421**, 826 (2003).

[13] A. S. Alnaser, T. Osipov, E. P. Benis, A. Wech, B. Shan, C. L. Cocke, X. M. Tong, and C. D. Lin, Phys. Rev. Lett. **91**, 163002 (2003).

[14] F. Legare, I. V. Litvinyuk, P. W. Dooley, F. Quere, A. D. Bandrauk, D. M. Villeneuve, and P. B. Corkum, Phys. Rev. Lett. **91**, 093002 (2003).

[15] A. S. Alnaser, B. Ulrich, X. M. Tong, I. V. Litvinyuk, C. M. Maharjan, P. Ranitovic, T. Osipov, R. Ali, S. Ghimire, Z. Chang, C. D. Lin, and C. L. Cocke, Phys. Rev. A **72**, 030702(R) (2005).

[16] Th. Ergler, A. Rudenko, B. Feuerstein, K. Zrost, C. D. Schroter, R. Moshammer, and J. Ullrich, Phys. Rev. Lett. **95**, 093001 (2005).
[17] Th. Ergler, B. Feuerstein, A. Rudenko, K. Zrost, C. D. Schroter, R. Moshammer, and J. Ullrich, Phys. Rev. Lett. **97**, 103004 (2006).
[18] K. F. Lee, F. Legare, D. M. Villeneuve, and P. B. Corkum, J. Phys. B **39**, 4081 (2006).
[19] W. A. Bryan, E. M. L. English, J. McKenna, J. Wood, C. R. Calvert, I. C. E. Turcu, R. Torres, J. L. Collier, I. D. Williams, and W. R. Newell, Phys. Rev. A **76**, 023414 (2007).
[20] Y.-H. Chen, S. Varma, A. York, and H. M. Milchberg, Opt. Express **15**, 11341 (2007).
[21] I. V. Litvinyuk, K. F. Lee, P. W. Dooley, D. M. Rayner, D. M. Villeneuve, and P. B. Corkum, Phys. Rev. Lett. **90**, 233003 (2003).
[22] D. Pavicic, K. F. Lee, D. M. Rayner, P. B. Corkum, and D. M. Villeneuve, Phys. Rev. Lett. **98**, 243001 (2007).
[23] J. Itatani, D. Zeidler, J. Levesque, M. Spanner, D. M. Villeneuve, and P. B. Corkum, Phys. Rev. Lett. **94**, 123902 (2005).
[24] N. Wagner, X. Zhou, R. Lock, W. Li, A. Wüest, M. Murnane, and H. Kapteyn, Phys. Rev. A **76**, 061403(R) (2007).
[25] V. Kumarappan, L. Holmegaard, C. Martiny, C. B. Madsen, T. K. Kjeldsen, S. S. Viftrup, L. B. Madsen, and H. Stapelfeldt, Phys. Rev. Lett. **100**, 093006 (2008).
[26] H. Mashiko, C. M. Nakamura, C. Li, E. Moon, H. Wang, J. Tackett, and Z. Chang, Appl. Phys. Lett. **90**, 161114 (2007).
[27] A. S. Alnaser, X. M. Tong, T. Osipov, S. Voss, C. M. Maharjan, B. Shan, Z. Chang, and C. L. Cocke, Phys. Rev. A **70**, 023413 (2004).
[28] B. Feuerstein and U. Thumm, Phys. Rev. A **67**, 063408 (2003).
[29] Th. Ergler, A. Rudenko, B. Feuerstein, K. Zrost, C. D. Schroter, R. Moshammer, and J. Ullrich, Phys. Rev. Lett. **97**, 193001 (2006).
[30] X. M. Tong, Z. X. Zhao, A. S. Alnaser, S. Voss, C. L. Cocke, and C. D. Lin, J. Phys. B **38**, 333 (2005).
[31] P. W. Dooley, I. V. Litvinyuk, K. F. Lee, D. M. Rayner, M. Spanner, D. M. Villeneuve, and P. B. Corkum, Phys. Rev. A **68**, 023406 (2003).
[32] X. M. Tong, Z. X. Zhao, and C. D. Lin, Phys. Rev. A **66**, 033402(R) (2002).
[33] A. S. Alnaser, C. M. Maharjan, X. M. Tong, B. Ulrich, P. Ranitovic, B. Shan, Z. Chang, C. D. Lin, C. L. Cocke, and I. V. Litvinyuk, Phys. Rev. A **71**, 031403 (2005).
[34] A. Apalategui and A. Saenz, J. Phys. B **35**, 1909 (2002).
[35] X. Urbain, B. Fabre, V. M. Andrianarijaona, J. Jureta, J. H. Posthumus, A. Saenz, E. Baldit, and C. Cornaggia, Phys. Rev. Lett. **92**, 163004 (2004).
[36] B. Feuerstein, Th. Ergler, A. Rudenko, K. Zrost, C. D. Schroter, R. Moshammer, J. Ullrich, T. Niederhausen, and U. Thumm, Phys. Rev. Lett. **99**, 153002 (2007).